

Full Paper

Development of Carbon-based Electrochemical Immunosensor for Detection of Anti-Newcastle Disease Virus Antibodies

**Imane Smaini, Raja Maallah, Mustapha Oukbab,* Mohamed Oubaouz,
Mohamed Amine Smaini, Rachida Najih, and Abdelilah Chtaini**

*Molecular Electrochemistry & Inorganic Materials Team, Faculty of Science and Technology,
Sultan Moulay Slimane University, Morocco*

*Corresponding Author, Tel.: +212 651575344

E-Mail: mustapha.oukbab@usms.ma

Received: 2 June 2025 / Received in revised form: 11 August 2025 /

Accepted: 16 September 2025 / Published online: 30 September 2025

Abstract- In this work, we developed a sensitive and selective immunosensor for the rapid and accurate detection of antibodies against the Newcastle disease virus. The sensor was fabricated using a carbon paste electrode modified with a secondary antibody–HRP conjugate immobilized via adsorption. The detection mechanism is based on electrical changes induced by biological interactions. Key physical parameters influencing current density were investigated and optimized. The modified electrode exhibited a good linear response to varying concentrations of Newcastle disease virus antibodies, as evaluated primarily using cyclic voltammetry (CV) and square wave voltammetry (SWV).

Keywords- Electrochemical sensor; Modified electrodes; Immunosensor; Carbon paste electrode; Newcastle disease virus; Antibody detection; Cyclic voltammetry; Square wave voltammetry; Linear response; Electrochemical impedance spectroscopy

1. INTRODUCTION

The concept of biosensors emerged from the need for real-time analysis without sample pre-treatment and without handling hazardous materials [1]. The market and applications of biosensors are broad, encompassing not only the medical field for diagnostics [2,3] but also environmental sanitary analysis [4] and food processing [5–9]. The development of biosensors began in the 1960s with the introduction of the first enzyme electrodes. Their expansion

accelerated in the 1980s with the commercialization of amperometric biosensors for glucose measurement, and by the 1990s, they found widespread use in medical diagnostics. To date, over 40 biosensors have been commercialized for medical applications, measuring parameters such as glucose, cholesterol, urea, and lactate levels [10]

Three main classes of biomolecules are commonly used as recognition elements [11]: enzymes, immunospecies (antibodies and antigens), and nucleic acids. Immunosensors, based on immunospecies, detect analytes via physical changes in the sensitive layer caused by the formation of immune complexes—these include changes in geometry, mass, and electrical properties [12–14]. Immunosensors are particularly amenable to miniaturization.

Recently, innovative nanomaterials have demonstrated significant potential to enhance detection sensitivity [9]. These nanomaterials possess unique properties, such as high surface-to-volume ratios and the ability to accelerate electron transfer between electrodes and immunospecies, thus improving sensor performance. Various nanomaterials have been explored, including gold nanoparticles, carbon nanotubes, and graphene [15,16].

In this work, we present a sensitive and selective immunosensor for detecting antibodies against the Newcastle disease virus. The sensor operation relies on electrical changes induced by biological interactions, specifically the binding between a peroxidase-secondary antibody conjugate (HRP-conjugate) and Newcastle disease virus-specific antibodies. The sensor performance was mainly evaluated using cyclic voltammetry (CV), square wave voltammetry (SWV), and electrochemical impedance spectroscopy (EIS) in the presence of NaCl as the electrolyte medium.

2. EXPERIMENTAL SECTION

2.1. Apparatus

The electrochemical experiments were conducted by a voltalab potentiostat (PGSTAT 100 model, Eco Chemie B.V., Utrecht, The Netherlands) controlled by the voltalab master 4 software. The carbon paste electrode was used as the working electrode (TE); the saturated calomel electrode (SCE) as the reference electrode (RE) and a platinum plate was used as the counter electrode (CE). The pH meter (Copenhagen, PHM210, Tacussel, French) was used to adjust the pH values [17].

2.2. Reagents and chemicals

2.2.1. Carbon graphite

The commercial graphite powder was supplied from France (Carbone, Lorraine, reference 9900). This powder was used in its raw state; it did not undergo any purification or pretreatment beforehand.

2.2.2. The peroxidase-secondary antibody conjugate (HRP-conjugate)

The chosen conjugate is a polyclonal antibody linked to HRP and commonly used in the Elisa test kit. It is intended for the detection of anti-pr-E antibodies of the Newcastle virus in the sera of horses and birds; it is obtained by the company ID.VET INNOVATIVE DIAGNOSTICS.

2.2.3. The positive serum contains Newcastle virus antibodies.

The positive serum contains Newcastle virus antibodies used in the Elisa test kit is also obtained by company ID.VET INNOVATIVE DIAGNOSTICS.

2.3. Preparation of the working electrode

The carbon paste electrode (CPE) is prepared by mixing graphite powder with a non-conductive binder, kerosene, in a mortar until a homogeneous paste is obtained [18]. Then, the paste is manually inserted into the cylindrical cavity of the electrode body (geometrical surface of about 0.1256 cm²). The electrical contact is established with a carbon rod.

2.4. Modification of the working Electrodes with Peroxidase-Secondary Antibody (PAS) Conjugate (HRP-Conjugate).

A solution of the peroxidase-secondary antibody conjugate (PAS) was prepared by diluting the concentrated conjugate in 2 mL of distilled or deionized water. The working electrode was then immersed in this conjugate solution for varying durations of 5, 10, 15, 30, and 60 minutes. During immersion, the solution was continuously stirred using a magnetic stir bar rotating at a constant speed to ensure homogeneous mixing [18-21].

The modified electrodes were electrochemically characterized at different interaction times using cyclic voltammetry (CV) and square wave voltammetry (SWV) techniques to determine the optimal deposition time of the peroxidase-secondary antibody conjugate on the electrode surface [19,20]. Additionally, the surface morphology of the selected electrode was examined using reflected light optical microscopy.

3. RESULTS AND DISCUSSION

3.1. Electrochemical Characterization of the Carbon Electrode Before and After Modification with the Secondary Peroxidase-Antibody Conjugate

Figure 1 presents the cyclic voltammograms of the electrodes: the bare carbon paste electrode (CPE, referred to as the working electrode before modification) and the modified electrode (CPE-NP—peroxidase-secondary antibody conjugate) in a NaCl electrolyte at pH 7. Comparing the voltammograms of the two electrodes, it is evident that the bare electrode (CPE) was successfully modified. This modification is indicated by an increase in the electrode's

electroactivity, attributed to the formation of a film of the peroxidase-secondary antibody conjugate on its surface. The oxidation scan reveals a peak centered at approximately 0.6 V.

The square wave voltammograms (Figure 1, part II) differ significantly between the two electrodes, reflecting changes in surface morphology and further confirming the successful modification of the electrode by the peroxidase-secondary antibody conjugate.

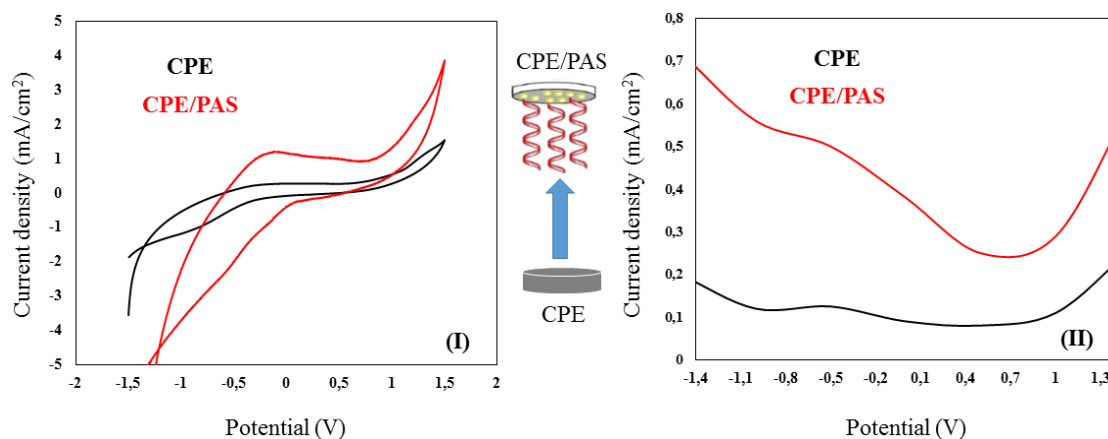


Figure 1. Superposition of cyclic voltammograms (I) and square wave voltammograms (II) of (a) unmodified CPE and (b) CPE modified with the peroxidase–secondary antibody conjugate, recorded in 0.1 M NaCl; scan rate: 100 mV/s; potential range: –2 V to 2 V; pH = 7

3.2. Optimization of Adsorption Parameters

3.2.1. Choice of Deposition Time

To determine the optimal deposition time of the peroxidase-antibody conjugate on the electrode surface, the electrode was immersed for different durations (0, 5, 15, and 30 minutes) in a solution of the peroxidase-secondary antibody conjugate at a fixed concentration. Figure 5 shows the overlay of the cyclic voltammetry (CV) and square wave voltammetry (SWV) voltammograms of the carbon paste electrode (CPE) modified with the peroxidase-secondary antibody conjugate at these various deposition times [21].

After electrochemical characterization of the modified electrodes, the current density was plotted as a function of the contact time between the CPE and the peroxidase-secondary antibody conjugate (Figures 2 and 3).

Between 2 and 10 minutes of immersion, an increase in current density was observed, indicating the initial formation of a layer on the electrode surface. At 30 minutes, the current density plateaued, suggesting that a stable film of the peroxidase-secondary antibody conjugate had formed. Therefore, 30 minutes was selected as the optimal deposition time for all subsequent experiments to maximize sensor response.

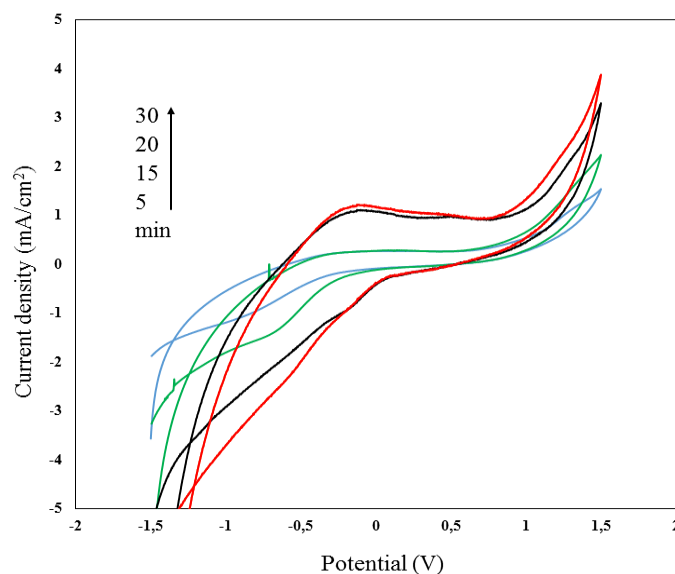


Figure 2. Superposition of cyclic voltammograms of CPE modified with the peroxidase–secondary antibody conjugate at different deposition times, recorded in 0.1 M NaCl; scan rate: 100 mV/s; potential range: –2 V to 2 V; pH = 7

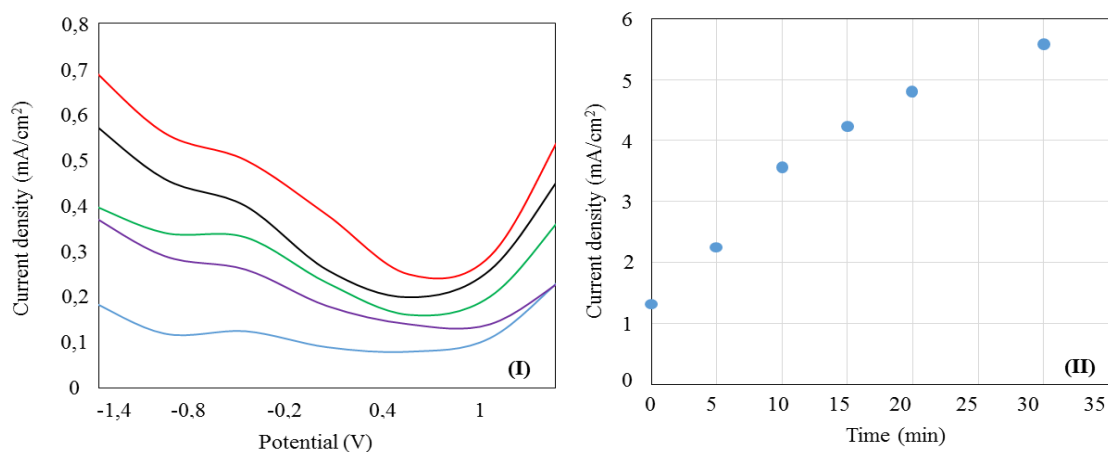


Figure 3. Current density as a function of the contact time between the CPE/PAS electrode and the peroxidase-secondary antibody conjugate solution

3.2.2. Electrochemical study the effect of antibody incubation time

The CPE-PAS immunosensor was incubated with an antibody solution for different durations. During the first 30 minutes of contact, the anodic peak current density increased rapidly with incubation time, reflecting enhanced electroactivity at the electrode surface due to the reaction between the antibodies and the peroxidase-secondary antibody conjugate, specifically the formation of bonds between the antibodies and the secondary antibodies.

Therefore, 30 minutes was chosen as the optimal incubation time to maximize the signal while minimizing the analysis duration.

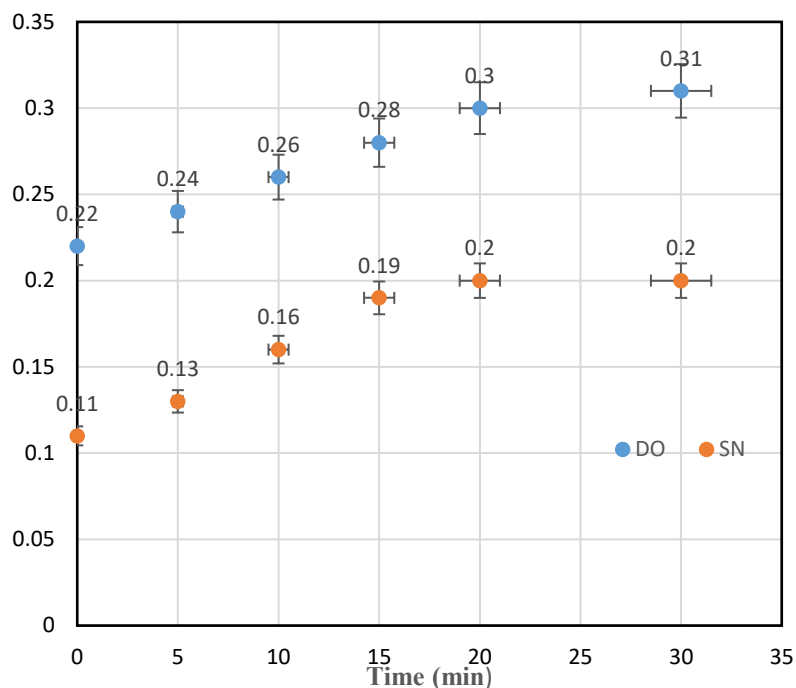


Figure 4. Optical density as a function of contact time between CPE/PAS and antibodies

We observe that both optical density (OD) and S/N increase with the contact time of CPE/PAS with the antibodies, which corresponds to a decrease in the antibody concentration in the solution. This decrease can be explained by the adsorption of antibodies onto the electrode surface.

For each sample, the signal-to-noise ratio percentage (% S/N) was calculated as follows:

$$S/N = \frac{\text{DO \acute{e}chantillon}}{\text{DO}_{\text{CN}}} \times 100$$

- Samples with S/N less than or equal to 40% are considered positive.
- Samples with S/N between 40% and 50% are considered indeterminate (or inconclusive).
- Samples with S/N greater than 50% are considered negative.

3.2.3. Electrochemical study of CPE/PAS

The carbon paste electrode modified by adsorption with the peroxidase-secondary antibody conjugate (CPE/PAS) was electrochemically characterized in the presence of antibodies. Figure 5 presents the cyclic voltammograms recorded in NaCl solution (0.1 M, pH 7) for the modified electrode in the presence of antibodies (positive serum, Figure 5I) and in their absence (negative serum, Figure 5II). The presence of antibodies is indicated by the appearance of an oxidation peak at approximately 0.2 V on the voltammogram.

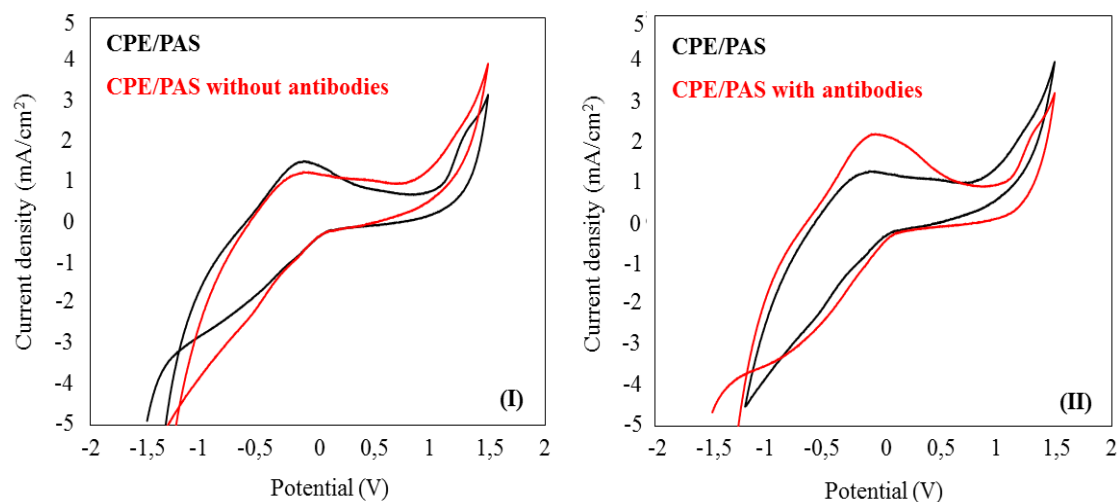


Figure 5: Superposition of cyclic voltammograms of CPE/PAS without antibody (I – negative serum) and CPE/PAS with antibody (II – positive serum), in 0.1 M NaCl; $v = 100$ mV/s, from -2 V to 2 V; pH = 7

The mechanism we propose for this process is schematized as follows:

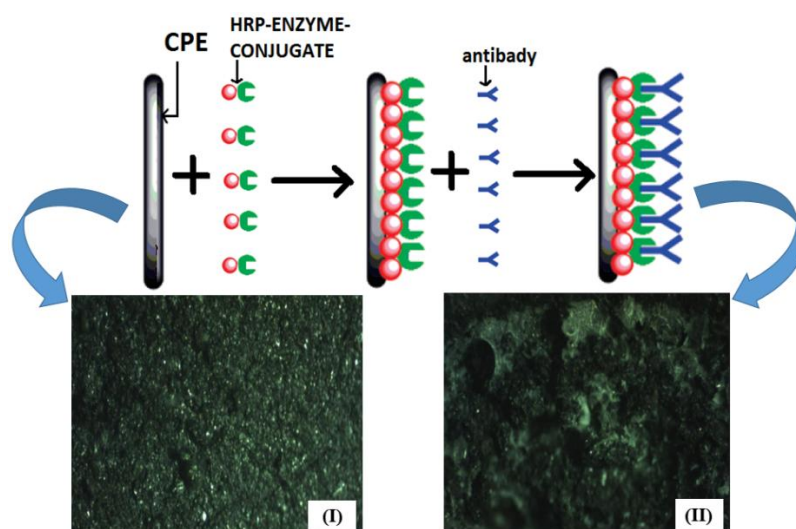


Figure 6. Schematic representation of the preparation of the immunodetection layer: Electrode CPE/PAS before incubation with antibodies (I) and after 20 minutes of incubation with antibodies (II)

3.2.4. Study of the sweep rate effect on CPE / PAS in the presence of antibodies

Figure 7 shows cyclic voltammograms recorded using the CPE modified with the peroxidase-secondary antibody conjugate at different potential scan rates. Although the overall shape of the voltammograms remains unchanged, the influence of scan rate is evident in the variation of peak current densities and their corresponding potentials.

As the scan rate increases, the peak current density also increases, and the oxidation potential shifts toward more positive (anodic) values. This behavior suggests that at higher scan rates, more electroactive sites become accessible on the electrode surface.

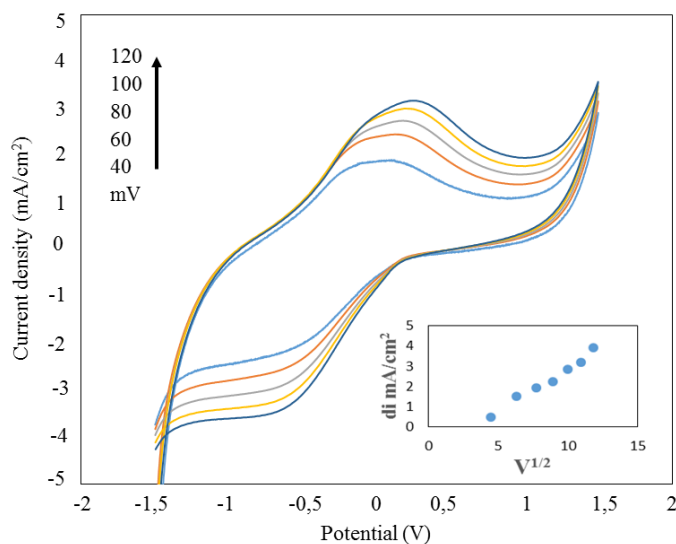


Figure 7. Superposition of cyclic voltammograms of CPE-NP/PAS at different scan rates (60, 80, 100, 120, 140, and 160 mV/s) in 0.1 M NaCl; potential range: -2 V to 2 V

3.2.5. Study of the effect of antibody concentration

The immunosensor was incubated in different media containing increasing concentrations of antibodies for 20 minutes. As shown in Figure 8, an increase in current density was observed with increasing antibody concentration. This indicates that the sensor's detection capability improves as the antibody loading increases, up to concentration C4.

- At low antibody concentrations, the signal is low but detectable. The immobilized antibodies do not fully cover all active sites on the electrode surface.
- At higher concentrations, the signal increases significantly, indicating specific adsorption of antibodies onto the conjugate layer.
- A slight saturation trend is observed at concentrations above C4, likely due to the saturation of available binding sites on the electrode surface.

3.2.6. Calibration Curve

The calibration curve illustrates that the cathodic peak current intensity recorded on the CPE/PAS immunosensor is proportional to the optical density (OD) of the antibodies, as determined by the classical ELISA method, within the concentration range from C6 to C1 (see Figure 9). This linear relationship is expressed by the following equation:

$$D_i = -3,010 D_O + 2,129 \quad R^2 = 0,993$$

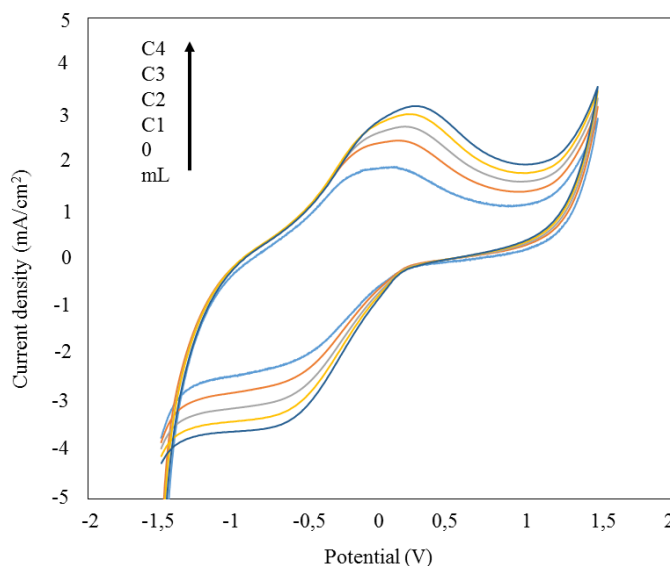


Figure 8. Superposition of cyclic voltammograms of modified CPE at different concentrations of peroxidase-secondary antibody conjugate in 0.1 M NaCl; scan rate: 100 mV/s; potential range: -2 V to 2 V; pH = 7

Table 1. Influence of antibody concentration on the intensity of reduction peaks obtained by CV on the surface of CPE-NP / PAS

ECH	C1	C2	C3	C4	C5	C6	C7
Current density (mA/cm ²)	0.7	0.79	0.87	0.97	1.04	1.13	1.22
DO	0.4768	0.4454	0.4124	0.3897	0.3598	0.3257	0.3086

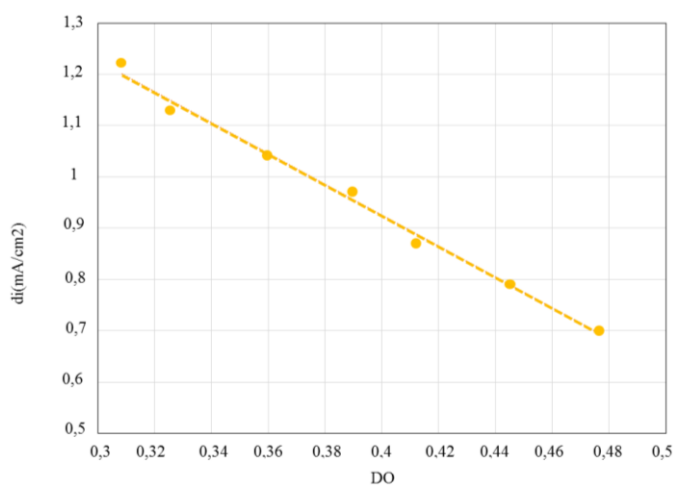


Figure 9. Determination of the detection and quantification limits of the CPE/PAS immunosensor

According to Miller and Miller [2], the standard deviation of the measured mean current (SD) can be modeled by the equation:

$$SD = \frac{1}{(n-2)} \sum_{j=1}^n (i_j - I_j)^2$$

Where i_j is the experimental value of the current measured during experiment j , and I_j is the corresponding value calculated at the same optical density using the calibration equation. n represents the number of measurements performed. The calculated standard deviation (SD) is then used to determine the Limit of Detection (LOD) and Limit of Quantification (LOQ). For the antibody-modified carbon paste electrode, the calculated values are presented in Table 2, showing the LOD and LOQ for the detection of Newcastle disease virus antibodies:

Table 2. Limits of Detection (LOD) and Quantification (LOQ)

LD	3 × SD/slope	2.34 10⁻³
LQ	10 × SD/slope	8.64 10⁻⁴

4. CONCLUSION

We developed a sensitive and selective immunosensor for the rapid and accurate detection of antibodies against the Newcastle disease virus, using a carbon paste electrode modified with a secondary antibody–HRP conjugate immobilized by adsorption. To optimize the performance of this biosensor, we investigated several key parameters, including the optimal deposition time of the secondary antibody–HRP conjugate on the electrode surface, the incubation time of the modified electrode with the target antibodies, and the effect of antibody concentration on the signal quality. The main objective of this study was to develop a system capable of reliably detecting antibodies in serum, offering analytical performance comparable to that of established methods such as ELISA, while providing additional advantages—namely simplicity of fabrication, rapid response, reusability through simple handling, and significantly lower cost.

Acknowledgments

I would like to thank the Molecular Electrochemistry and Inorganic Materials team of the Sultan Moulay Slimane University in Beni Mellal (Morocco).

Declarations of interest

The authors declare that they have no known competing financial interests or personal relationships that could have appeared to influence the work reported in this paper.

Credit authorship contribution statement

Imane Smaini: Conceptualization, Methodology, Writing – original draft. **Raja Maallah** Conceptualization, Methodology, Writing – original draft. **Mustapha Oukbab:** Data curation, Writing– review & editing, Software. **Mohamed Oubaouz:** Data curation, Writing– review & editing, Software. **Mohamed Amine Smaini:** Data curation, Writing– review & editing, Software. **Rachida Najih:** Data curation, Writing–review & editing, Software. **Abdelilah. Chtaini:** Validation, Resources, Supervision.

REFERENCES

- [1] K. Bizet, *Immunoassay & Specialized Biology* 10 (1995) 205.
- [2] E.C. Alocilja, and S.M. Radke, *Biosensors and Bioelectronics* 18 (2003) 841.
- [3] N. Madhura, et al., *Biosensors and bioelectronics* 25 (2009) 661.
- [4] S.V. Dzyadevych, et al. *Sensors and Actuators B: Chemical* 105 (2005) 81.
- [5] B.M. Paddle, *Biosensors and Bioelectronics* 11 (1996) 1079.
- [6] C. Michel, et al. *Biosensors and Bioelectronics* 22 (2006) 285.
- [7] L.D. Mello, and L.T. Kubota, *Food Chemistry* 77 (2002) 237.
- [8] A. Amine, et al. *Biosensors and Bioelectronics* 21 (2006) 1405.
- [9] V. Venugopal, *Biosensors and bioelectronics* 17 (2002) 147.
- [10] P. Binder, *Immunoassay & Specialized Biology* 5 (1990) 23.
- [11] V. Velusamy, et al. *Biotechnology advances* 28 (2010) 232.
- [12] J. Castillo, et al. *Sensors and Actuators B: Chemical* 102 (2004) 179.
- [13] B. Mohamed, M. Boitard, and N. El Murr, *Biosensors and Bioelectronics* 14 (1999) 545.
- [14] C.A. Anton, C. Negulescu, and R.P. Baldwin, *Biosensors and Bioelectronics* 18 (2003) 303.
- [15] A.P. Girard-Egrot, et al. *Colloids and Surfaces B: Biointerfaces* 23 (2002) 319.
- [16] R. Maallah, et al. *Sensing and Bio-Sensing Research* 24 (2019) 100279.
- [17] R. Maallah, A. Moutcine, and A. Chtaini. *Biosens. Bioelectron.* 7 (2016) 2155.
- [18] R. Maallah, et al. *American International Journal of Biology and Life Sciences* 1 (2019) 1.
- [19] M.A. Smaini, et al. *Biol. Syst. Open Access* 6 (2017) 173.
- [20] A. Moutcine, et al. *J. Material. Sci. Eng.* 5 (2016) 2169.
- [21] M.A. Smaini, R. Maallah, I. Smaini, et al. *J. Immunol. Tech. Infect. Dis.* 10 (2021) 2.